

Thermodynamic and structural aspects of the potential energy surface of simulated water

Francis W. Starr^{1,2}, Srikanth Sastry³, Emilia La Nave¹, Antonio Scala^{1,4},
H. Eugene Stanley¹, and Francesco Sciortino⁴

¹*Center for Polymer Studies, Center for Computational Science, and Department of Physics, Boston University, Boston, MA 02215 USA*

²*Polymers Division and Center for Theoretical and Computational Materials Science, National Institute of Standards and Technology, Gaithersburg, MD, 20899 USA*

³*Jawaharlal Nehru Centre for Advanced Scientific Research, Jakkur Campus, Bangalore 560064, INDIA*

⁴*Dipartimento di Fisica e Istituto Nazionale per la Fisica della Materia, Università di Roma “La Sapienza”, Piazzale Aldo Moro 2, I-00185, Roma, ITALY*

(28 July 2000)

Relations between the thermodynamics and dynamics of supercooled liquids approaching a glass transition have been proposed over many years. The potential energy surface of model liquids has been increasingly studied since it provides a connection between the configurational component of the partition function on one hand, and the system dynamics on the other. This connection is most obvious at low temperatures, where the motion of the system can be partitioned into vibrations within a basin of attraction and infrequent inter-basin transitions. In this work, we present a description of the potential energy surface properties of supercooled liquid water. The dynamics of this model has been studied in great details in the last years. Specifically, we locate the minima sampled by the liquid by “quenches” from equilibrium configurations generated via molecular dynamics simulations. We calculate the temperature and density dependence of the basin energy, degeneracy, and shape. The temperature dependence of the energy of the minima is qualitatively similar to simple liquids, but has anomalous density dependence. The unusual density dependence is also reflected in the configurational entropy, the thermodynamic measure of degeneracy. Finally, we study the structure of simulated water at the minima, which provides insight on the progressive tetrahedral ordering of the liquid on cooling.

PACS numbers: 61.43.Fs, 64.70.Pf, 66.10.Cb

I. INTRODUCTION

In recent years, numerical study of model liquids in supercooled states has been helpful to clarify the physics of the glass transition [1]. The availability of long trajectories in phase space offers the possibility of closely examining the changes in supercooled states that are responsible for slowing down the dynamics by 15 decades in a narrow temperature range approaching the glass transition. Although current computational studies are limited to times shorter than $\approx 1 \mu\text{s}$ (as opposed to real liquids, for which the dynamics can be studied up to $\approx 10^2 \text{ s}$), a coherent picture of the glass transition phenomenon is beginning to emerge.

In addition to characterizing changes in the dynamics, recent studies have demonstrated the utility of examining the underlying potential energy surface (PES) as an aid to understanding the properties of supercooled liquids connecting the dynamics to the thermodynamics and the topology of configuration space [2–9]. This connection is most obvious at low temperatures, where the motion of the system can be partitioned into motion confined within a single potential energy basin with infrequent inter-basin transitions. It has been shown that at sufficiently high temperature (at constant volume), the

system explores always the same distribution of basins, and that the average basin energy is nearly temperature independent. Below a crossover temperature—which is coincident with the onset of a two-step relaxation in the decay of density fluctuations [2]—the system starts to populate basins of progressively lower energy, but which are less numerous.

The thermodynamic approach based on the analysis of the PES, following the formalism proposed by Stillinger and Weber [10], has become a powerful formalism for the interpretation of numerical data, both in equilibrium [2–9] and in out-of-equilibrium conditions [11,12]. The degeneracy of the energy minima, i.e., the number of basins with a selected minimum energy, has been quantified for several model systems and used to calculate the configurational entropy S_{conf} , from which an “ideal” glass transition (in the sense of Kauzmann, Adam, Gibbs, and DiMarzio [13–15]) has been estimated [4,5,7,9].

In this paper we present a detailed investigation of the properties of local potential energy minima, or “inherent structures” (IS), sampled by the extended simple point change (SPC/E) model of water [16]. Previous studies on the PES for models of water have shown the relevance of this approach to the deepening of our understanding of both structural and dynamical properties of liquid wa-

ter [7,17–23]. Specifically, we calculate the temperature and density dependence of the basin energy over a wide range of temperatures and densities. We also study in detail the shape of the basins in configuration space and estimate their degeneracy. The information presented provides a detailed characterization of the PES and furnishes all information required to explicitly write the liquid Helmholtz free energy in a wide temperature and density range. Finally, we study the geometrical arrangement of the molecules at IS minima to better understand the changes that take place in the liquid on cooling. Focusing on the IS allows us to eliminate thermal effects which complicate the temperature dependence. In particular, we focus on the fraction of water molecules that are four-coordinated.

II. SIMULATIONS

The majority of the state points studied here are from the molecular dynamics simulations of the SPC/E model performed in Ref. [24]. The simulation methods are discussed in Ref. [24]. We have performed additional simulations of ice I_h , so that we can compare the IS properties of the crystal with those of the liquid. The simulations of ice consist of a periodic box containing 432 molecules with dimensions $2.634 \text{ nm} \times 2.281 \text{ nm} \times 2.151 \text{ nm}$ for density $\rho = 1.0 \text{ g/cm}^3$. The dimensions are uniformly scaled in order to obtain other densities. The box dimensions have been optimized to generate the lowest energy configuration at density 1.0 g/cm^3 . Proton disorder in the initial configuration is generated by identifying closed hydrogen bond loops, and exchanging hydrogens between molecules, as described in Ref. [25].

The ice simulations have been performed at $\rho = 0.90, 0.95, 1.00$, and 1.05 g/cm^3 and temperature $T = 194 \text{ K}$. The thermodynamic properties are summarized in Table I. The equilibration time for these sample is far less than that of the liquid at the same temperature since only the vibrational degrees of freedom need to be relaxed.

We have performed conjugate gradient minimizations [26] to locate local minima on the PES closest to any given instantaneous configuration. We use a tolerance of 10^{-15} kJ/mol in the total energy for the minimization. For each state point, we quench at least 100 configurations taken from two independent trajectories. While each configuration is not necessarily separated by the typical relaxation time of the system, the set of points quenched typically spans ≈ 25 times the relaxation time of the intermediate scattering function.

III. INHERENT STRUCTURE PROPERTIES OF SPC/E

A. Thermodynamics in the Inherent Structure Formalism

Stillinger and Weber formalized the concept of a basin in the potential energy surface by introducing the inherent structure formalism [10]. The set of points that map to the same minimum via steepest descent are those which constitute a basin, and the minimum of a basin is the IS. This approach is particularly well suited to simulated liquids, since it is possible to explicitly calculate the steepest descent trajectory from an equilibrium state point. Moreover, the partition function Z can be explicitly written in terms of the basins. In the isochoric-isothermal (NVT) ensemble, for a system of N rigid molecules

$$Z = \lambda^{-6N} \int \exp(-V/k_B T) d^N \mathbf{r} \quad (1)$$

which can be written as a sum over all basins in configurational space, i.e.

$$Z = \lambda^{-6N} \sum_{\text{basins}} \exp(-e_{IS}/k_B T) \times \int_{R_{\text{basin}}} \exp(-(V - e_{IS})/k_B T) d^N \mathbf{r}. \quad (2)$$

Here $\lambda \equiv h(2\pi m k_B T)^{-1/2}$ is the de Broglie wavelength, $V \equiv V(\mathbf{r}^N)$ is the potential energy as a function of the atomic coordinates, e_{IS} is the energy of the IS and R_{basin} is the configuration space associated to a specific basin. The model system we consider here, namely SPC/E water, has six degrees of freedom for each molecule. It is natural to introduce $\Omega(e_{IS})$, the number of minima with energy e_{IS} , and the free energy of a basin with basin energy e_{IS} $f(T, e_{IS})$ (the “basin free energy”).

$$f(T, e_{IS}) \equiv -k_B T \ln \left(\frac{1}{\Omega(e_{IS})} \lambda^{-6N} \times \sum_{\text{basins}}^* \int_{R_{\text{basin}}} \exp[-(V - e_{IS})/k_B T] d^N \mathbf{r} \right), \quad (3)$$

The asterisk denotes the fact that the sum is constrained to basins of energy e_{IS} . Eq. (3) accounts for both the basin structure surrounding the minimum and the kinetic degrees of freedom. The complete partition function can be written as the sum over all possible e_{IS} values,

$$Z = \sum_{e_{IS}} \Omega(e_{IS}) \exp \left(-\frac{e_{IS} + f(T, e_{IS})}{k_B T} \right) \quad (4)$$

or

$$Z = \sum_{e_{IS}} \exp \left(-\frac{-TS_{\text{conf}}(e_{IS}) + e_{IS} + f(T, e_{IS})}{k_B T} \right) \quad (5)$$

where the configurational entropy $S_{\text{conf}}(e_{IS}) \equiv k_B \ln(\Omega(e_{IS}))$. In the thermodynamic limit, the corresponding Helmholtz free energy $F(T, V)$ is given by

$$F(V, T) = E_{IS}(T) + f(T, E_{IS}(T)) - TS_{\text{conf}}(E_{IS}(T)) \quad (6)$$

where $E_{IS}(T)$ is the thermodynamic average of e_{IS} and solves

$$\begin{aligned} \partial F(V, T)/\partial e_{IS} &= 1 + \partial f(T, e_{IS})/\partial e_{IS} - \\ T\partial S_{\text{conf}}(T, e_{IS})/\partial e_{IS} &= 0. \end{aligned} \quad (7)$$

$E_{IS}(T)$ can be numerically calculated by estimating the IS which are populated by a system in equilibrium at temperature T and fixed volume V . Hence, if a good model for $f(T, e_{IS})$ is available, then the e_{IS} dependence of S_{conf} along isochores can be estimated by integrating Eq. (7). Note that Eq. (7) shows that, if the basin free energy does not depend on e_{IS} , then the configurational entropy is the only quantity controlling the T -dependence of E_{IS} . In other words, the statistical mechanics of the basins completely decouples from the vibrational dynamics [27,28].

$S_{\text{conf}}(E_{IS})$ can also be calculated by studying the probability distribution $P(E_{IS}, T)$, i.e. the probability that the liquid—in equilibrium at temperature T —populates the inherent structure E_{IS} . Indeed, from Eq. (5)

$$S_{\text{conf}}(e_{IS}) = k_B \ln P(e_{IS}, T) + e_{IS}/T + f(e_{IS}, T) + k_B \ln Z(T). \quad (8)$$

Hence, Eq. 8 gives S_{conf} up to an unknown constant $k_B \ln Z(T)$. This “histogram technique” has been recently used to estimate the configurational entropy for a binary-mixture Lennard-Jones system [4,6,9,29].

B. Inherent Structure Energy as a function of ρ and T

The ρ - and T -dependence of E_{IS} for the SPC/E potential for a more limited range of T was recently reported in Ref. [22]. Our results for the IS energies are shown in Fig. VI(a) as a function of ρ and in Fig. VI(b) as a function of T .

The IS energy of the liquid along isotherms shows hints of negative curvature for $T \lesssim 230$ K (Fig. VI(a)). The presence of this negative curvature can also be observed in the instantaneous equilibrium configurations [30]. This curvature yields a *negative* contribution to compressibility [30] $K_T^{-1} = V[(\partial^2 U/\partial V^2)_T - T(\partial^2 S/\partial V^2)_T]$, which might be related to a low-temperature critical point in SPC/E [31]. Fig. VI also shows the IS energy for ice I_h (which coincides with the ground state energy). At the lowest T studied, E_{IS} of the disordered liquid is still significantly greater than that of ice [32]. Note that ice I_h is not the thermodynamically stable crystalline form for SPC/E [33], and the stable SPC/E crystal would most likely have a lower ground state energy. However, the stable SPC/E crystal does not correspond to any of the experimentally-known forms of ice [34]. Fig VI(a) also

show the Kauzmann energy E_K , which we discuss in sec. IIID.

Fig. VI(b) shows that at high T , E_{IS} is nearly T independent. For $T \lesssim 350 - 400$ K, there is a rapid decrease of E_{IS} with a weak density-dependence. At low T , E_{IS} depends linearly on $1/T$, as shown in Fig. VI(c). The $1/T$ dependence of E_{IS} can be derived from the partition function provided $\Omega(e_{IS})$ is Gaussian, and that the basin free energy does not depend on e_{IS} [5,28]. Furthermore, as found for the Lennard-Jones liquids [2], the T at which the IS energy starts to decrease correlates with the temperature at which a two-step relaxation starts to be observed in all characteristic correlation functions (see, e.g., Fig. 13 of Ref. [24])

C. The Basin Free Energy: Density of States

We next focus on the shape of the IS basin with the aim of developing a model for the basin free energy. In the harmonic approximation, the basin free energy is given by

$$F(E_{IS}, T) = k_B T \sum_{i=1}^{6N-3} [\ln(\hbar\omega_i/k_B T)], \quad (9)$$

the free energy of a harmonic oscillator with frequency spectrum ω_i . The values ω_i^2 are the eigenvalues of the Hessian matrix, defined by the second derivative of the potential energy with respect to the molecular degrees of freedom at the basin minimum. The mass and moments of inertia of a molecule have also been absorbed in the definition of ω_i . The distribution of ω_i , called the density of states (DOS), is shown in Fig. VI(a) for three different state points at $T = 210$ K. The pronounced minimum at $\omega \approx 400$ cm^{-1} separates the translational modes (at lower frequencies) from the rotational modes (at higher frequencies). At larger ρ , the peaks in the DOS broaden due to the disruption of the H-bond network, which we will discuss in Sec. IV. For comparison, we also show the DOS for ice I_h , where we see a clear separation between the translational and rotational modes.

The normal mode spectrum contributes to the basin free energy via the term $6\langle \ln(\hbar\omega) \rangle$ (per molecule), where the brackets denote an average over the DOS and over different configurations. The dependencies on both T and ρ of $\langle \ln(\hbar\omega) \rangle$ are shown in Fig. VI(b). The dependence of $6k_B \langle \ln(\hbar\omega) \rangle$ on E_{IS} is shown in Fig. VI(c). The average basin frequency is larger in deeper basins, showing that the basins become increasingly “sharp” on cooling. This is in contrast with the Lennard Jones case, where the basins become broader on cooling [11,12]. The average curvature of the IS basin at high density has a weaker E_{IS} -dependence (and hence T -dependence) than those at low density, but are generally larger than the curvature at low density.

Fig. VI shows the harmonic free energy estimate of Eq. (9) as a function of ρ . The range of values of the vibrational free energy of Fig. VI (6 to 9 kJ/mol) is not very different from the range of values of E_{IS} of Fig. VI(a) (from -55 to -60 kJ/mol); thus both make a significant contribution to the free energy of Eq. (6).

The basin free energy estimated using the harmonic approximation of Eq. (9) can be used as a starting point for estimating the true basin free energy. For a more precise quantification of the basin free energy, we must consider anharmonic contributions to the free energy. Indeed the basins of the SPC/E are anharmonic. This can easily be seen by considering the difference $U_{\text{vib}} \equiv U - E_{IS}$; for a molecular system in the harmonic approximation, $U_{\text{vib}} = (6/2)k_B T$. Fig. VI shows a marked deviation from harmonic behavior. However, as we discuss next, the anharmonicity does not have a strong E_{IS} dependence. Development of techniques for the estimation of the anharmonic contribution to the basin free energy would be very useful.

D. Basin Degeneracy

A key element in the description of the configuration space in the IS thermodynamic formalism is $\Omega(e_{IS})$, the number of basins with energy e_{IS} . The corresponding configurational entropy S_{conf} —i.e. the logarithm of $\Omega(e_{IS})$ —can be calculated by integrating Eq. (7). Using the harmonic approximation of Eq. (9) for the basin free energy, we obtain

$$S_{\text{conf}}(E_{IS}) = S_{\text{conf}}(E_0) + \int_{E_0}^{E_{IS}} \frac{dE_{IS}}{T} + \quad (10)$$

$$k_B \langle \ln(\omega(E_{IS})/\omega(E_0)) \rangle. \quad (11)$$

Fig. VI(a) separately shows the contribution from $\int dE_{IS}/T$, and the contribution associated with $\langle \ln(\omega(E_{IS})/\omega(E_0)) \rangle$. The harmonic contribution is not negligible. To obtain the S_{conf} in absolute scale, the value of S_{conf} at the reference point E_0 is needed. We have used reference values obtained in Ref. [7] by independently calculating the absolute value of the entropy via thermodynamic integration from the known ideal gas reference point.

The complete results for all densities are shown in Fig. VI(b). In the same graph we show a fit to $S_{\text{conf}}(E_{IS})$ using the form

$$S_{\text{conf}}(E_{IS}) = A(E_{IS} - E_K)^2 + B(E_{IS} - E_K) \quad (12)$$

where E_K , the Kauzmann energy, is the E_{IS} value at which the configurational entropy vanishes. This functional form is equivalent to the Gaussian distribution of $\Omega(e_{IS})$ [5]. The resulting E_{IS} values, which provide an indication of the ρ dependence of E_K , are reported in Fig. VI(a). The E_K values suggest that disordered states with energies comparable to the ordered crystalline states

may be available to this system [22], provided the E_K estimates are not significantly affected by unknown errors in the extrapolation procedure or in the reference value for $S_{\text{conf}}(E_0)$ used.

To confirm independently the validity of the approach followed to estimate E_{IS} dependence of S_{conf} , we compare the value obtained from Eq. (10) with the value obtained using Eq. (8) in Fig. VI(c). The agreement between the curves is remarkable. Moreover, the overlap for different $P(e_{IS}, T)$ distributions after the harmonic E_{IS} dependence is taken into account, suggests that there are no other systematic E_{IS} -dependent contributions. Any remaining T -dependent contributions are absorbed in the unknown $Z(T)$ function.

The results reported in this section provide a detailed analysis of the inherent structures and of their basins. This information can be used to develop a detailed free energy expression for the SPC/E [31]. Calculation of the T dependence of S_{conf} was presented in Ref. [7], to probe the relation between the configurational contributions to thermodynamic quantities and the liquid dynamics in supercooled states.

IV. STRUCTURE

On lowering T the dramatic changes in the IS energies are known to be accompanied by equally dramatic changes in the dynamic properties of the instantaneous configurations. However, examination of simple measures of structure of the instantaneous configurations (such as the pair distribution function) do not reveal such obvious changes; rather, there is a very gradual change, with the structure becoming slowly more well defined. A more careful analysis of structure is required to see significant changes [35]. In the following, we focus our attention on the structural changes that can be observed by studying the IS to try to obtain a more clear picture of the structural evolution of the system on cooling. The results we present are complementary to the results recently reported for the same system along similar lines of thought [22] and expand on previous work [20,36].

A. Pair distribution function

Fig. VI shows the oxygen-oxygen pair correlation function for both the equilibrated liquid and for the inherent structures at various T and ρ . We first focus our attention on the T dependence along the $\rho = 1.00$ g/cm³ isochore. For equilibrated configurations as well as inherent structures, the first and second peaks of the pair correlation function become better defined upon decreasing the temperature. Further, there is a systematic reduction of the intensity between the first and second neighbor peaks. At higher density ($\rho = 1.40$ g/cm³), the behavior

is somewhat different; for the instantaneous configurations, there is a clear T dependence, while for the IS, the T dependence is nearly negligible. For comparison, the model atomic liquid studied in [2,4], shows virtually no T dependence of $g(r)$ in the IS (Fig 7). Hence the behavior at large ρ is more like that expected for a simple liquid, consistent with the disappearance at large ρ of many of the anomalies that differentiate water at ambient density.

We also show the behavior of $g(r)$ for various ρ at $T = 210$ K in the bottom panels of Fig. VI. On increasing ρ , both the instantaneous and inherent structure configurations show an increase in intensity at $r \approx 0.32$ nm, a trait already known to develop due to distortion (and eventual interpenetration) of the hydrogen bond network. For water, it is known that the preferred nearest-neighbor geometry is tetrahedral. This tetrahedral ordering is obvious at low densities, where peaks at 0.28 nm and 0.45 nm are the expected distances for a perfect tetrahedral lattice with first neighbor separation of 0.28 nm. To see more clearly the tetrahedral nature of the liquid at all these temperatures and densities, we focus on the neighbor statistics at the various state points.

B. Neighbor Changes

We first consider the the average number of neighbors that a molecule has within a sphere of radius r , which is obtained from integration of $g(r)$:

$$n(r) = 4\pi\rho \int_0^r r'^2 g(r') dr'. \quad (13)$$

We show $n(r)$ in Fig. 8 as a function of ρ at the lowest T studied. We see a plateau in $n(r)$ almost exactly equal to four for all densities. Therefore, even at large ρ , the liquid has short range tetrahedral order. However, the rapid growth of $n(r)$ at large ρ highlights the distortion and interpenetration.

To quantify the T dependence of the structural changes we calculate the distribution of the number of neighbors a molecule has within a distance 0.31 nm (arrow in Fig. 8), roughly corresponding to the first minimum in $g(r)$ at low density, shown in Fig. VI. We choose the first minimum in $g(r)$ at low density to emphasize the tetrahedrality of the liquid; for ice, all molecules would have 4 neighbors, while in high density liquid configurations, the distortion leads to a significant number of molecules having more or less than 4 neighbors in the first shell. Fig. 9 shows the histograms of the fraction of molecules with a given coordination number. At low density, the histogram for the instantaneous configurations changes from a rather broad one to one that is peaked around the value 4 as the temperature decreases, as we expect. The same trend is visible for the inherent structures, although even at high temperatures, the distribution is quite narrowly peaked around the value 4. Such a comparison permits us to make a separation between

deviations from four-coordination arising from thermal agitation, and that arising from configurational change. This less marked T dependence of the IS can be seen for all ρ . At larger ρ , the distribution is still peaked around 4, but there is significant fraction of molecules which are not four-bonded — these are molecules most likely participating in the so called *bifurcated bonds* [20].

To quantify the changes in the tetrahedrality as a function of T for each ρ , we plot the fraction of four-bonded molecules f_4 as a function of T in Fig. 10. Those molecules which are not four bonded represent the set of bifurcated bonds [20]. At low density, it is interesting to note that for both the equilibrated configurations and inherent structures, this f_4 is close to 1 at the lowest T simulated. Indeed, for T somewhat lower than we can currently simulate, it appears that all molecules would be four bonded, and hence form a perfect random tetrahedral network. A simple extrapolation of f_4 for the lowest densities, displayed in Fig. 11, shows that $T(f_4 = 1)$ appears slightly lower than the mode-coupling transition temperature T_{MCT} [24,37,38] but well above T_K . Additionally, it appears that both the instantaneous and IS configurations appear to reach a random tetrahedral network at roughly the same temperature. The close correspondence of $T(f_4 = 1)$ and T_{MCT} suggests that this crossover in structural change may be the controlling mechanism for the crossover in dynamic properties at T_{MCT} [8,39,40]. However, the extrapolation does not allow us to unambiguously associate these temperatures. Since the tetrahedral geometry is the “ideal” configuration at these low densities, there are unlikely to be any significant structural changes in the liquid for $T < T(f_4 = 1)$; to the extent that there is further structural change for $T < T(f_4 = 1)$, the rate of change must be significantly different than for $T > T(f_4 = 1)$. Analysis of the neighbor statistics in the IS at lower T might shed some light on the hypothesized change in the dynamics from that of a fragile liquid to a strong liquid [41–43], a widely debated topic [44].

At larger densities increases, it is apparent that a random tetrahedral network is never reached. This is apparent in the fact that there are far fewer four-bonded molecules in the first neighbor shell at the higher densities. Hence, no sharp change in the structural development as a function of T is expected. Consequently any crossover from fragile to strong behavior must become less pronounced.

V. CONCLUSIONS

We have characterized the properties of the PES basins in the configuration space of the SPC/E model over a range of densities in the supercooled regime. We have shown that the T dependence of E_{IS} is qualitatively very similar to the previous observations of simple liquids. We have also shown the importance of accounting for the

shape of the basins when characterizing the thermodynamic properties of the IS subsystem. In particular, we found there are significant T dependent anharmonic effects. This detailed information on the basins should be useful for any future studies that focus on the dynamics of exploring the PES, or the thermodynamics at low T . Such a classification of basin properties would also be useful for other model glass formers, and might help to highlight the differences between fragile (such as OTP) and strong (such as SiO_2) glass formers [45].

In addition, we presented results for the structural changes of the IS; these changes are more pronounced than what can be seen from equilibrium configurations. In particular, the progression of the structure toward a random tetrahedral network at low T holds promise for a more physical and intuitive understanding of the glass transition in water. Below the temperature of crossover to a tetrahedral network, no further structural arrangement is expected, and the configurational entropy of the liquid may be nearly “frozen in” at the value that corresponds to the random tetrahedral network (plus the residual defects that would be present at concentrations varying with density). Thus the rate of change in entropy of the liquid may be expected change substantially near the crossover temperature, resulting in a significantly lower value of T_K , compared to the value that may be expected if the rate of change above the crossover temperature persisted. Similarly, because of the significant temperature dependence of the fraction of bifurcated bonds – which facilitate structural rearrangement – above the cross-over temperature, and the relative constancy below, the temperature dependence of the dynamical properties may show a corresponding crossover.

Finally, we call attention on the possibility of studying physical aging in this model-system, starting from the thermodynamic description of this system. We note that, at $\rho = 1.40 \text{ g/cm}^3$, there is almost no variation of the basin curvature (Fig. VI) on E_{IS} , nor does the structure change significantly (Fig. VI). Hence these high density state points may offer an ideal opportunity to check if the out-of-equilibrium dynamics at very low T can be still related to equilibrium states of the system [12].

VI. ACKNOWLEDGMENTS

We thank P.G. Debenedetti, S.G. Glotzer, and F.H. Stillinger for helpful discussions. F.W.S. is supported by the National Research Council. F.S. is supported by INFM-PRA-HOP and *Iniziativa Calcolo Parallelo* and from MURST PRIN 98. This work was also supported by the NSF.

- [1] See for example K. Binder et al., in *Complex Behaviour of Glassy Systems*, M. Rubí and C. Perez-Vicente Eds. (Springer Berlin 1997); W. Kob, J. Phys-Condens. Mat. **11**, R85 (1999).
- [2] S. Sastry, P.G. Debenedetti, and F.H. Stillinger, Nature **393**, 554 (1998).
- [3] L. Angelani, G. Parisi, G. Ruocco and G. Viliani, Phys. Rev. Lett. **81**, 4648 (1998).
- [4] F. Sciortino, W. Kob, and P. Tartaglia, Phys. Rev. Lett. **83**, (1999).
- [5] A. Heuer, Phys. Rev. Lett. **78**, 4051 (1997); S. Buechner and A. Heuer, Phys. Rev. E. **60**, 6507 (1999).
- [6] B. Coluzzi, P. Verrochio, and G. Parisi, Phys. Rev. Lett **84**, (2000).
- [7] A. Scala, F.W. Starr, E. La Nave, F. Sciortino, and H.E. Stanley, Nature **406**, 166 (2000).
- [8] T.B. Schröder, S. Sastry, J. Dyre and S.C. Glotzer, J. Chem. Phys. **112**, 9834 (2000)
- [9] S. Sastry, Phys. Rev. Lett. **85**, 590 (2000).
- [10] F.H. Stillinger and T.A. Weber, Phys. Rev. A **25**, 978 (1982); Science **225**, 983 (1984). F. H. Stillinger, Science, **267**, 1935 (1995).
- [11] W. Kob, F. Sciortino, and P. Tartaglia, Europhys. Lett. **49**, 590 (2000).
- [12] F. Sciortino and P. Tartaglia, cond-mat/0007208
- [13] A.W. Kauzmann, Chem. Rev. **43**, 219 (1948).
- [14] J. H. Gibbs and E. A. DiMarzio, J. Chem. Phys. **28**, 373 (1958).
- [15] G. Adams and J.H. Gibbs, J. Chem. Phys. **43**, 139 (1965)
- [16] H. J. C. Berendsen, J. R. Grigera, and T. P. Stroatsma, J. Phys. Chem. **91**, 6269 (1987).
- [17] F.H. Stillinger and T.A. Weber, J. Phys. Chem **87**, 2833 (1983); F. H. Stillinger and T. Head-Gordon Phys. Rev. E **47**, 2484 (1993)
- [18] I. Ohmine and H. Tanaka, Chem. Rev. **93**, 2545 (1993). I. Ohmine, H. Tanaka, P.G. Wolynes, J. Chem. Phys. **89**, 5852 (1988); H. Tanaka and I. Ohmine, J. Chem. Phys **91**, 6318 (1989).
- [19] F. Sciortino, A. Geiger and H.E. Stanley, Phys. Rev. Lett. **65**, 3452 (1990).
- [20] F. Sciortino, A. Geiger, and H. E. Stanley, Nature **354** 218 (1991); F. Sciortino, A. Geiger, and H. E. Stanley, J. Chem. Phys. **96**, 3857 (1992).
- [21] M. Cho, G.R. Fleming, S. Saito, I. Ohmine and R. Stratt, J. Chem. Phys. **100**, 6672 (1994).
- [22] C.J. Roberts, P.G. Debenedetti, and F.H. Stillinger, J. Phys. Chem B **103**, 10258 (1999).
- [23] M. Sasai, Physica A (in press).
- [24] F.W. Starr, S. Harrington, F. Sciortino, and H.E. Stanley, Phys. Rev. Lett. **82**, 3629 (1999); F.W. Starr, F. Sciortino, and H.E. Stanley, Phys. Rev. E **60**, 6757 (1999).
- [25] A. Rahman and F.H. Stillinger, J. Chem. Phys. **57**, 4009 (1972).
- [26] W. H. Press, B. P. Flannery, A. A. Teukolsky and W. T. Vetterling, *Numerical Recipes - The Art of Scientific Computing* (Cambridge University, Cambridge, 1986).
- [27] F. Sciortino, W. Kob and P. Tartaglia, Proceedings of *Unifying Concepts in Glass Physics, Trieste, 1999*, J. Phys. Cond. Mat. **12**, 6525 (2000).

- [28] R. J. Speedy, *J. Phys. Chem. B* **103**, 4060 (1999).
- [29] S. Sastry, Proceedings of *Unifying Concepts in Glass Physics, Trieste, 1999*, *J. Phys. Cond. Mat.* **12**, 6515 (2000).
- [30] S.T. Harrington, P.H. Poole, F. Sciortino, and H.E. Stanley, *J. Chem. Phys.* **107**, 7443 (1997).
- [31] A. Scala, F.W. Starr, E. La Nave, H.E. Stanley, and F. Sciortino, cond-mat/0007488.
- [32] In ref. [22] the IS energy of the liquid at 230 K was found to be lower than that of the estimated ice Ih ground state energy for $\rho \lesssim 0.95 \text{ g/cm}^3$ and $\rho \gtrsim 1.05 \text{ g/cm}^3$. In contrast, our results show that ice Ih is at a significantly lower energy than the liquid IS at a lower temperature of 210 K. This is most likely explained by the fact that our results are direct calculation of the IS energy, while the results of Ref. [22] are only an estimation of the ground state energies.
- [33] L.A. Baez and P. Clancy, *J. Chem. Phys.* **103**, 9744 (1995); *Mol. Phys.* **86** 385 (1995).
- [34] N. H. Fletcher, *The Chemical Physics of Ice* (Cambridge Univ. Press, Cambridge, 1970).
- [35] H. Jonsson and H. C. Andersen *Phys. Rev. Lett.* **60**, 2295 (1988).
- [36] F. W. Starr, S. Sastry, F. Sciortino and H. E. Stanley, Proceedings of the DAE Solid State Physics Symposium 1999 (in press); cond-mat/0001296.
- [37] P. Gallo, F. Sciortino, P. Tartaglia, and S.-H. Chen *Phys. Rev. Letts* **76**, 2730 (1996); F. Sciortino, P. Gallo, P. Tartaglia, and S.-H. Chen *Phys. Rev. E* **54**, 6331 (1996); F. Sciortino, L. Fabbian, S.-H. Chen, P. Tartaglia, *Phys. Rev. E* **56**, 5397 (1997); L. Fabbian, A. Latz, R. Schilling, F. Sciortino, P. Tartaglia, and C. Theis *Phys. Rev. E* **60**, 5768 (1999).
- [38] F. Sciortino, *Chem. Phys.* **258** 295 (2000).
- [39] F. Sciortino and P. Tartaglia, *Phys. Rev. Lett.* **78**, 2385 (1998).
- [40] E. La Nave, A. Scala, F.W. Starr, F. Sciortino, H.E. Stanley, *Phys. Rev. Lett.* **84**, 4605 (2000).
- [41] K. Ito, C. T. Moynihan and C. A. Angell *Nature* **398** 492 (1999); S. Sastry, *Nature* **398**, 467 (1999).
- [42] F.W. Starr, C. A. Angell, R. J. Speedy, and H. E. Stanley cond-mat/9903451.
- [43] R. Bergman and J. Swenson, *Nature* **403**, 283 (2000).
- [44] R.S. Smith, and B.D. Kay, *Nature* **398**, 288 (1999).
- [45] C. A. Angell, *J. Non-Cryst. Solids* **131-133**, 13 (1991).

TABLE I. Summary of the thermodynamics properties obtained from simulations of Ice Ih, all at $T = 194 \text{ K}$.

$\rho \text{ (g/cm}^3\text{)}$	P (MPa)	U (kJ/mol)
0.90	-560	-55.52
0.95	-77	-56.38
1.00	475	-56.34
1.05	700	-55.44

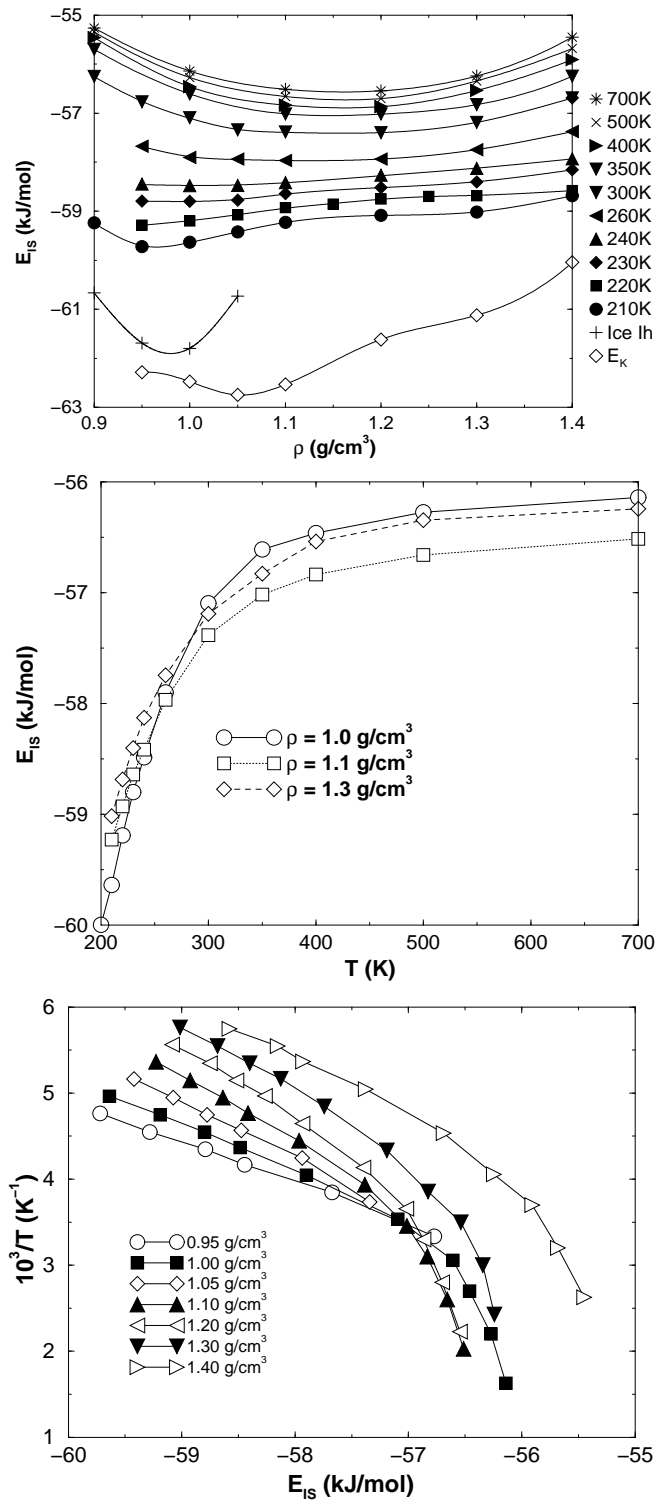


FIG. 1. Inherent structure energy. (a) Density dependence of the E_{IS} for liquid configurations, and ice Ih. The bottom curve is $E_K(\rho)$, obtained by fitting S_{conf} using Eq. (12). Note that the three lowest isotherms, as well as $E_K(\rho)$ display inflections. (b) T dependence of E_{IS} for selected densities. For $T \lesssim 400$ K, E_{IS} starts to decrease rapidly, corresponding to the fact that the systems populate basins of lower energy. (c) $1/T$ vs E_{IS} for all studied densities. The linear relationship at low T support the possibility that the e_{IS} values are Gaussian distributed. Curves for different densities have been shifted by multiplies of 0.2 for clarity.

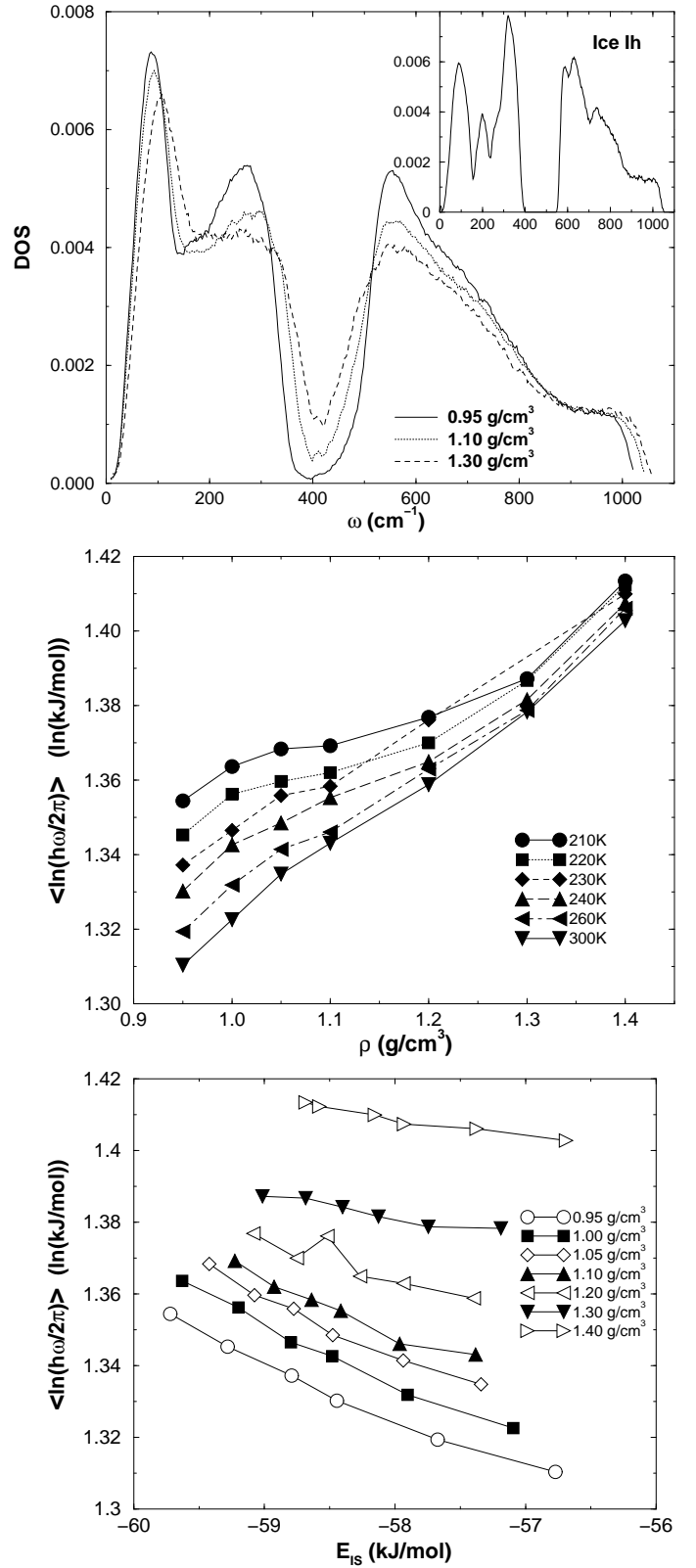


FIG. 2. Shape of the basins surrounding the inherent structure. (a) The DOS of the liquid at $T = 210$ K. The inset shows the DOS for ice Ih at $\rho = 1.00$ g/cm³ for comparison. (b) Change of harmonicity of the basins (c) $\langle \log(\hbar\omega) \rangle$ vs E_{IS} for different densities.

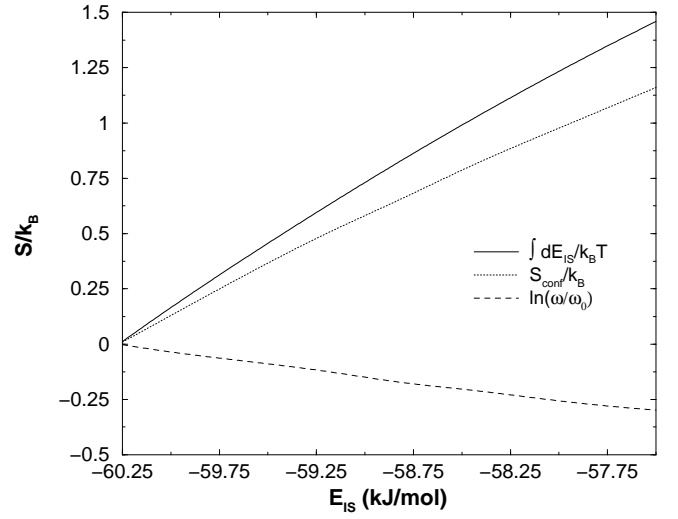
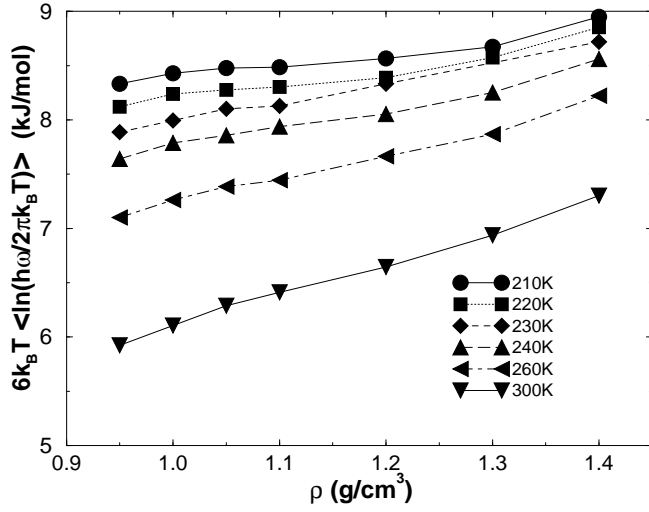


FIG. 3. Free energy of a basin in the harmonic approximation.

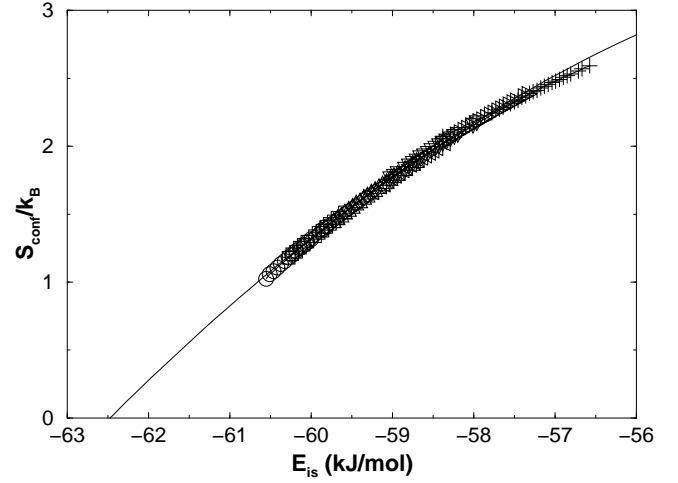
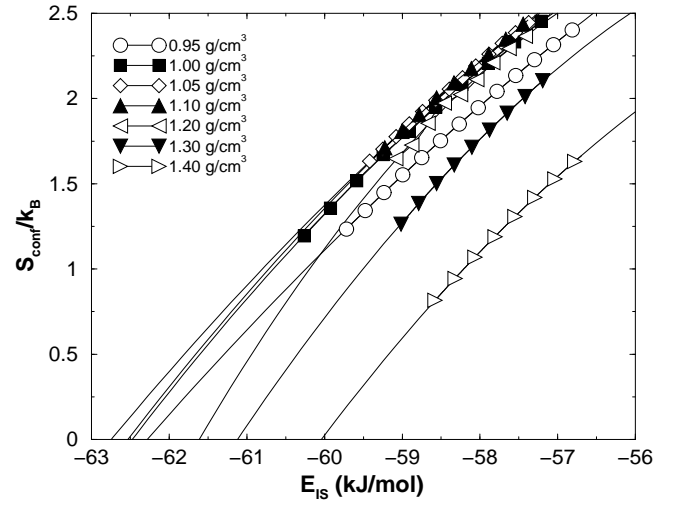
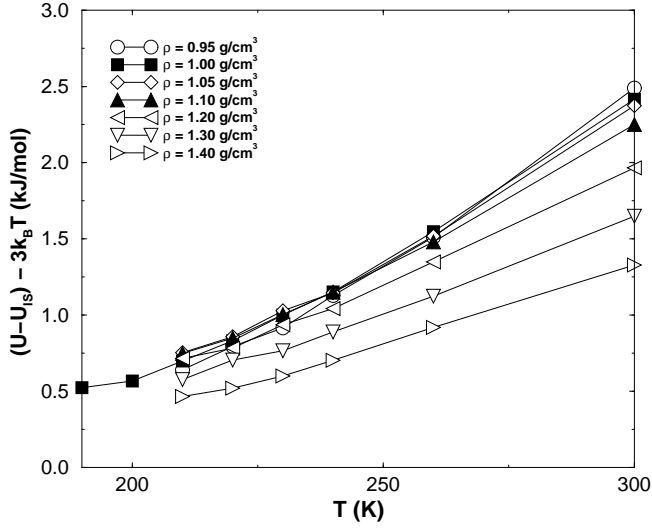


FIG. 4. Anharmonicity of the basins as a function of T .

FIG. 5. Configurational entropy S_{conf} . (a) Role of the different contributions in the estimate of S_{conf} . (b) E_{IS} -dependence of the configurational entropy for different ρ . Lines are extrapolation to lower E_{IS} value based on the assumption of linear relation between E_{IS} and $1/T$ at low T . (c) Comparison between the S_{conf} values obtained using Eq.8 and Eq.10 for $\rho = 1.0 \text{ g/cm}^3$. Symbols refer to different $P(E_{IS}(T), T)$ distributions, shifted to maximize the overlap for different T -values.

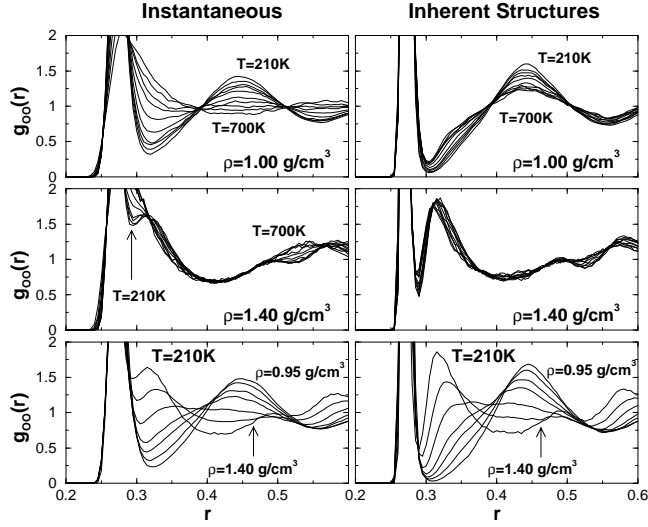


FIG. 6. Oxygen-oxygen pair correlation function, for equilibrated liquid configurations, and inherent structures. Upon lowering temperature, the first peak in both cases becomes sharper, and the intensity between the first and second peaks decreases. The smaller changes seen in the case of the inherent structures offers an estimate of that part of the change due to configurational change upon cooling, as opposed to thermal effects.

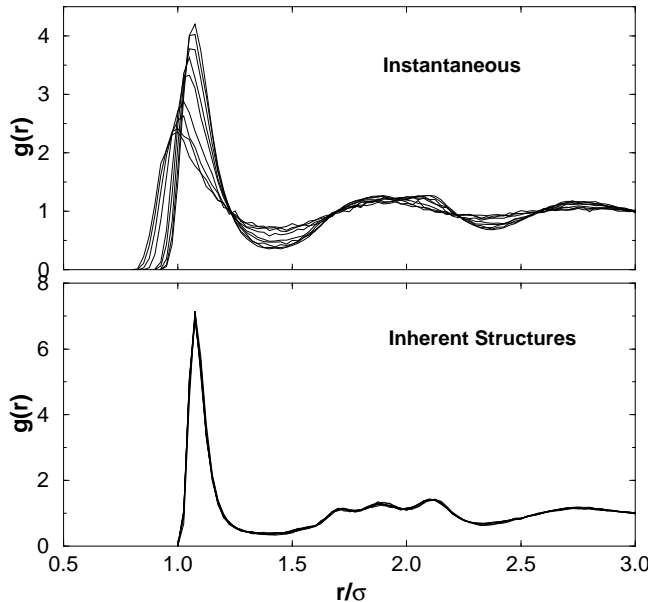


FIG. 7. Pair correlation function for equilibrated liquid configurations, and inherent structures of the frequently studied binary Lennard-Jones mixture between $T = 0.44$ and $T = 5$ in units of the pair potential energy depth [the model parameters are defined in Ref. [4]]. Upon lowering temperature, there is no apparent change in the structure of the IS, similar to the behavior we observe for water at large ρ .

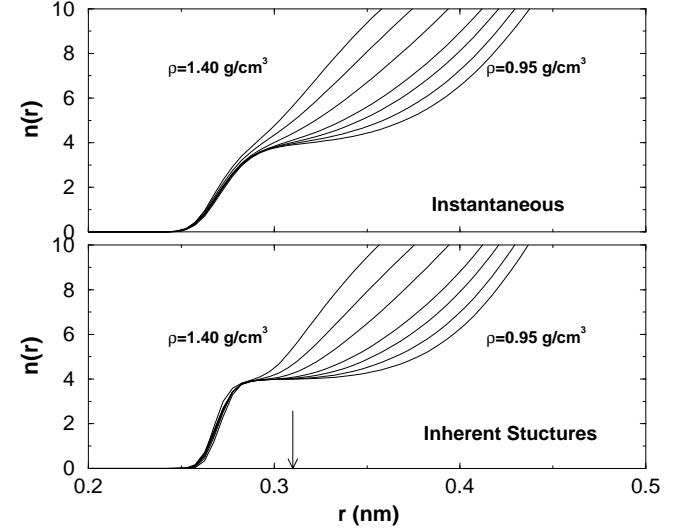


FIG. 8. Average number of neighbors $n(r)$ as a function of distance r . For all densities, an average of nearly four neighbors is reached at the first neighbor distance, showing the tendency for short range tetrahedral ordering, even at very high density.

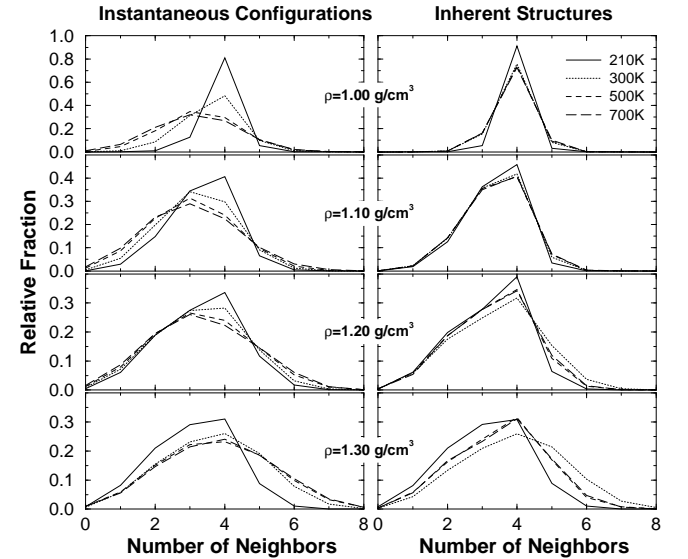


FIG. 9. Distribution of the coordination number of molecules for both the instantaneous equilibrated configurations, and the inherent structures. In all cases, the fraction of four-coordinated molecules increases with decreasing T .

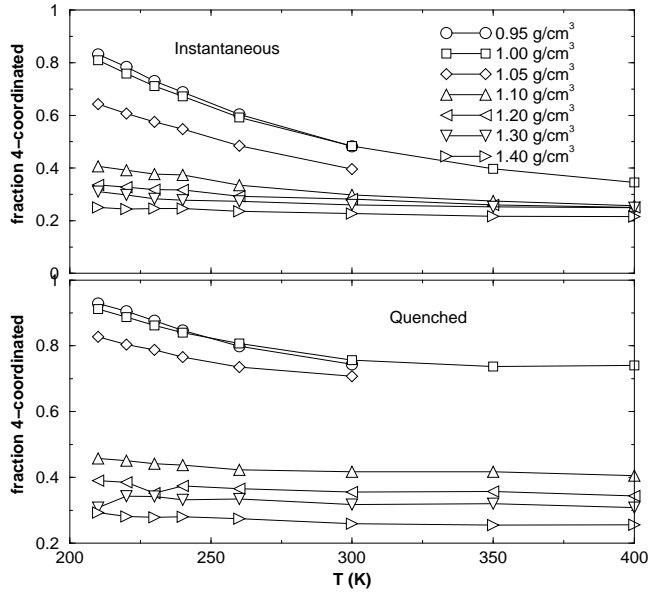


FIG. 10. Fraction of four coordinated water molecules: (a) equilibrated configurations and (b) inherent structures.

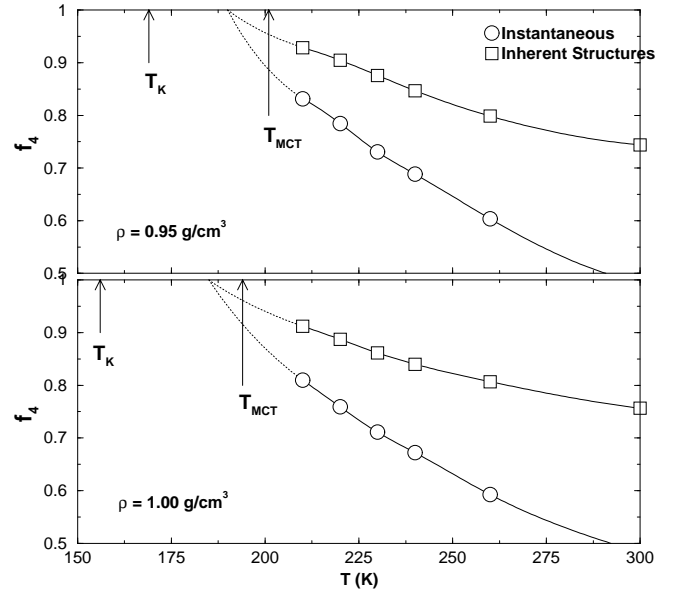


FIG. 11. Extrapolation for f_4 to lower T to estimate $T(f_4) = 1$.